JRB-74-201-AA

E7.4-10.399
CR-137224

USE OF SKYLAB EREP DATA IN A SEA SURFACE TEMPERATURE EXPERIMENT

Fourth Quarterly Report

David C. Anding
John P. Walker

Science Applications, Incorporated
Ann Arbor, Michigan 48103

Prepared for
National Aeronautics and Space Administration
Johnson Space Center
Houston, Texas 77058

Contract NAS9-13277

February 1974

jb associates

USE OF SKYLAB EREP DATA IN A SEA SURFACE TEMPERATURE EXPERIMENT

Fourth Quarterly Report

David C. Anding
John P. Walker

Science Applications, Incorporated
Ann Arbor, Michigan 48103

Prepared for

National Aeronautics and Space Administration
Johnson Space Center
Houston, Texas 77058

Contract NAS9-13277

February 1974

FOREWORD

The research described herein, which was conducted by JRB Associates - a wholly owned subsidiary of Science Applications, Incorporated, was performed under NASA Contract NAS9-13277. This fourth quarterly report covers the period from 17 November 1973 to 17 February 1974.

ABSTRACT

This report discusses the status of an experiment to utilize S191 spectrometer data acquired over ocean areas to assess the ability of spaceborne infrared multispectral sensing to function as a means of providing improved estimates of sea surface temperature over that obtainable with a single channel radiometric instrument. The data received from SL-2 and SL-3 are summarized and critiqued. No specific results pertinent to the final experimental objectives are presented.

Use of Skylab EREP Data in a Sea Surface Temperature Experiment

INTRODUCTION

NASA is planning to launch an ocean observation satellite in the near future (Nimbus G) which will contain a two-channel infrared radiometric instrument capable of measuring the sea surface temperature to an accuracy of ± 1 Kelvin. The initial design of the instrument has been postulated but the spectral response of each of the two channels has not been finalized. It is expected that the results of EREP will influence the spectral response selection. An experiment of particular relevance consists of acquiring S191 infrared spectrometer data ($\sim$6 to $\sim$15 μm) over ocean areas for which the atmospheric and sea surface conditions and temperatures are known. The measured data will be compared with theoretical predictions and postulated radiometric techniques for measuring sea surface temperatures will be tested. The results are expected to provide an important input to the final selection of the spectral response of each of the two radiometric channels. The status of this experiment is described herein.

During the first quarter of the investigation period a prelaunch effort was performed [1]. This involved the refinement of radiative transfer models and algorithms and the development of software required for the overall investigation. During the second and third quarters minimal effort was performed while awaiting receipt of Skylab data. During the period 12/1/73 to 1/7/74 all data from SL-2 and SL-3 were received. A summary of the data received, which lends itself readily to analysis, is given in table I.

The target area for pass 5 is the Gulf of Mexico immediately south of Houston. The target area for pass 8 is the southern central portion of the Gulf of Mexico approximately 350 miles south of New Orleans. For both of these SL-2 passes the S191 was locked at nadir. For each of the

Table I.

S191 Data Products Received for Which There Was Support Photography

Mission	Date	Pass	GMT Start	Lat.	Long.	GMT Finish	Lat.	Long.	No. Spectra
SL-2	6/5/73	5	18:03:05	27.8N	95.4W	18:03:35	26.5N	94.0W	33
SL-2	6/11/73	8	15:21:44	26.4N	89.2W	15:23:03	22.6N	85.2W	85
SL-3	8/8/73	16	15:57:19	45.3N	125.3W	15:58:49	45.3N	125.3W	98
SL-3	9/12/73	36	17:08:20	37.0N	76.2W	17:09:33	37.0N	76.2W	11
SL-3	9/15/73	43	18:01:49	27.4N	123.0W	18:03:32	27.4N	123.0W	110
SL-3	9/17/73	46	15:06:54	37.6N	76.6W	15:07:00	37.6N	76.6W	7

SL-3 passes the target area was acquired forward of the spacecraft and tracked to nadir or beyond. (The latitude and longitude given in the table is the target location.) For pass 16 the target area was offshore coastal clouds off the coast of Oregon. The target areas for passes 36, 43 and 46 were, respectively; water area in Chesapeake Bay, coastal stratus clouds off the California coast, and a water area in Chesapeake Bay near the mouth of the Rappahannock River. For each set of data the S191 Viewfinder/Tracking System (V/TS) photography was examined and those spectra were selected for which there was corresponding photography (the number of spectra selected are given in table I). Each spectrum was plotted and examined and those spectra containing spurious signals were removed. The remaining spectra were analyzed statistically as a precursor to performing analyses related to the specific experimental objectives.

The results of the statistical analysis are presented herein and indicate that the data are probably incorrect in some spectral regions and that further analysis be delayed until the cause of the errors are resolved and the data corrected.

DATA ANALYSIS

SL-2, EREP Pass No. 5

Day of Year: 156, June 5, 1973
Location (approximate): 27N; 95W
GMT Start: 18:03:05
GMT End: 18:03:35
Sun Angle (approximate): 60^{o}

Skylab was in a descending mode on EREP pass No. 5. For the target of concern V/TS photography began at 18:03:05 and continued for 30 seconds. Considerable amounts of scattered low cumulus clouds were in the area and it could not be ascertained from the photography, because of uncertainties in the magnification, if the S191 field of view was clear or contaminated by clouds. From the

composite set of data 33 spectra were selected and certain statistical parameters were evaluated. These included the average value ($\overline{L}$) and standard deviation (σ_L) at each wavelength. The results are given in table II. In figure 1 σ_L is plotted versus wavelength and compared with the NESR given in the EREP Investigators Data Book. Since variations in atmospheric absorption and emission, and variations in sea surface radiations all contribute to the variance in the observed S191 signal, the system noise level appears commensurate with predictions. However, certain other aspects of the data appear unrealistic. This is demonstrated in figure 2 where S191 data is compared with calculations.* The calculated values are based upon a radiative transfer model described in the first quarterly report [1] and atmospheric temperature, humidity and sea surface temperature data supplied by Duncan Ross of NOAA.

The scenario of the acquisition of the environmental data was as follows. The aircraft, flying in a northwest direction along the suborbital track, began its descent from approximately 21,400 feet at 1620 hours GMT. During the descent air temperature and dew point temperature were recorded with a dew point hygrometer. The aircraft descended to an altitude of approximately 500 feet at 1700 hours GMT. The aircraft then flew along the suborbital track at 500 feet altitude continuing to record air and dew point temperature. The sea surface temperature was also measured with a Barnes PRT-5 radiometer. The surface temperature remained fairly uniform at $26.5 \pm 0.2^{\circ}C$. The aircraft began its ascent to 21,000 feet 1918 hours GMT during which air and dew point temperature were again recorded. The temperature and humidity profiles for ascent and descent were averaged and smooth curves were fitted to the data. The

---

* The effects of ozone absorption and emission near 9.6 μm were intentionally neglected from these and all similar calculations in this report because ozone concentrations were not known.

Table II.

Statistics for SL-2 EREP Pass No. 5, 5 June 1973

λ	$\bar{L}$	$\bar{T}_{eff.}$	$L_{max.}$	$L_{min.}$	σ_L	$\bar{L}+\sigma_L$	$\bar{L}-\sigma_L$
6.020	7.164E-05	240.120	9.900E-05	4.500E-05	1.366E-05	8.531E-05	5.798E-05
6.140	8.236E-05	241.196	1.320E-04	4.900E-05	2.089E-05	1.032E-04	6.147E-05
6.260	1.167E-04	247.947	1.890E-04	7.900E-05	2.310E-05	1.398E-04	9.365E-05
6.390	1.317E-04	248.908	1.630E-04	9.200E-05	1.556E-05	1.473E-04	1.162E-04
6.510	1.020E-04	240.007	1.330E-04	7.300E-05	1.822E-05	1.203E-04	8.382E-05
6.640	1.156E-04	241.175	1.400E-04	9.600E-05	1.317E-05	1.288E-04	1.025E-04
6.780	1.531E-04	246.767	2.030E-04	1.300E-04	1.518E-05	1.683E-04	1.379E-04
6.910	1.922E-04	251.548	2.220E-04	1.520E-04	1.754E-05	2.097E-04	1.746E-04
7.050	2.322E-04	255.481	2.510E-04	2.100E-04	1.061E-05	2.428E-04	2.216E-04
7.190	2.785E-04	259.610	3.020E-04	2.480E-04	1.276E-05	2.913E-04	2.657E-04
7.340	3.056E-04	260.937	3.140E-04	2.850E-04	7.500E-06	3.131E-04	2.981E-04
7.480	3.407E-04	263.176	3.550E-04	3.250E-04	8.943E-06	3.497E-04	3.318E-04
7.630	3.867E-04	266.224	4.050E-04	3.560E-04	1.093E-05	3.977E-04	3.758E-04
7.790	3.837E-04	264.327	4.090E-04	3.660E-04	1.145E-05	3.951E-04	3.722E-04
7.940	4.364E-04	267.921	4.670E-04	4.120E-04	1.123E-05	4.477E-04	4.252E-04
8.100	5.269E-04	274.295	5.520E-04	5.080E-04	9.425E-06	5.363E-04	5.174E-04
8.260	6.479E-04	282.231	6.610E-04	6.270E-04	7.868E-06	6.557E-04	6.400E-04
8.430	7.105E-04	285.502	7.330E-04	6.870E-04	9.006E-06	7.195E-04	7.015E-04
8.600	7.284E-04	285.804	7.440E-04	6.970E-04	1.086E-05	7.393E-04	7.176E-04
8.770	7.551E-04	286.804	7.740E-04	7.300E-04	1.076E-05	7.659E-04	7.444E-04
8.940	7.695E-04	287.093	7.970E-04	7.350E-04	1.168E-05	7.812E-04	7.578E-04
9.090	7.827E-04	287.476	7.970E-04	7.690E-04	6.227E-06	7.889E-04	7.765E-04
9.120	7.842E-04	287.486	8.000E-04	7.530E-04	1.032E-05	7.945E-04	7.739E-04
9.270	7.774E-04	286.619	7.850E-04	7.680E-04	4.908E-06	7.823E-04	7.724E-04
9.300	7.744E-04	286.347	8.010E-04	7.610E-04	8.343E-06	7.828E-04	7.661E-04
9.460	6.877E-04	279.779	7.010E-04	6.710E-04	7.506E-06	6.952E-04	6.802E-04
9.490	6.708E-04	278.430	6.900E-04	6.520E-04	8.934E-06	6.797E-04	6.619E-04
9.650	5.926E-04	271.810	6.070E-04	5.800E-04	6.422E-06	5.990E-04	5.862E-04
9.650	5.895E-04	271.553	6.010E-04	5.730E-04	7.273E-06	5.968E-04	5.823E-04
9.840	6.081E-04	272.661	6.220E-04	5.880E-04	7.535E-06	6.156E-04	6.005E-04
10.040	7.142E-04	280.848	7.320E-04	6.960E-04	8.804E-06	7.230E-04	7.054E-04
10.070	7.328E-04	282.248	7.480E-04	7.120E-04	9.016E-06	7.418E-04	7.238E-04
10.240	7.991E-04	287.158	8.100E-04	7.850E-04	5.998E-06	8.051E-04	7.931E-04
10.270	8.018E-04	287.367	8.180E-04	7.890E-04	7.300E-06	8.091E-04	7.945E-04
10.440	8.060E-04	287.799	8.190E-04	7.870E-04	6.682E-06	8.127E-04	7.993E-04
10.480	8.076E-04	287.963	8.260E-04	7.920E-04	8.143E-06	8.158E-04	7.995E-04
10.650	8.019E-04	287.754	8.140E-04	7.920E-04	5.154E-06	8.071E-04	7.968E-04
10.680	8.061E-04	288.120	8.170E-04	7.960E-04	5.932E-06	8.121E-04	8.002E-04
10.870	7.994E-04	287.945	8.100E-04	7.920E-04	4.886E-06	8.042E-04	7.945E-04
10.900	8.002E-04	288.077	8.140E-04	7.890E-04	5.932E-06	8.062E-04	7.943E-04
11.080	7.941E-04	288.010	8.050E-04	7.780E-04	5.595E-06	7.997E-04	7.885E-04
11.100	7.832E-04	287.189	7.910E-04	7.720E-04	5.253E-06	7.885E-04	7.780E-04
11.200	7.950E-04	288.399	8.020E-04	7.800E-04	4.917E-06	7.999E-04	7.900E-04
11.310	7.929E-04	288.558	8.050E-04	7.830E-04	5.529E-06	7.985E-04	7.874E-04
11.350	7.827E-04	287.840	7.940E-04	7.690E-04	5.231E-06	7.879E-04	7.774E-04
11.530	7.838E-04	288.530	7.950E-04	7.750E-04	4.907E-06	7.887E-04	7.789E-04
11.760	7.656E-04	287.829	7.700E-04	7.600E-04	3.038E-06	7.687E-04	7.626E-04

Table II. (Continued)

λ	$\overline{L}$	$\overline{T}_{eff.}$	$L_{max.}$	$L_{min.}$	σ_L	$\overline{L}+\sigma_L$	$\overline{L}-\sigma_L$
12.000	7.508E-04	287.500	7.700E-04	7.410E-04	6.547E-06	7.574E-04	7.443E-04
12.240	7.313E-04	286.779	7.470E-04	7.190E-04	5.662E-06	7.369E-04	7.256E-04
12.480	6.915E-04	284.064	6.980E-04	6.820E-04	4.101E-06	6.956E-04	6.874E-04
12.730	6.803E-04	284.184	6.930E-04	6.640E-04	5.223E-06	6.855E-04	6.751E-04
13.400	5.572E-04	273.821	5.730E-04	5.410E-04	6.260E-06	5.635E-04	5.510E-04
13.600	5.054E-04	268.211	5.140E-04	4.970E-04	4.402E-06	5.098E-04	5.010E-04
13.800	4.856E-04	266.514	4.990E-04	4.730E-04	6.878E-06	4.925E-04	4.787E-04
14.000	4.496E-04	262.367	4.690E-04	4.380E-04	6.091E-06	4.557E-04	4.435E-04
14.100	4.363E-04	260.877	4.480E-04	4.260E-04	5.432E-06	4.418E-04	4.309E-04
14.200	4.189E-04	258.688	4.290E-04	4.090E-04	5.024E-06	4.239E-04	4.139E-04
14.300	3.992E-04	256.050	4.150E-04	3.900E-04	4.940E-06	4.042E-04	3.943E-04
14.400	3.866E-04	254.441	3.940E-04	3.770E-04	4.880E-06	3.915E-04	3.817E-04
14.500	3.810E-04	253.947	3.960E-04	3.690E-04	5.822E-06	3.868E-04	3.751E-04
14.600	3.697E-04	252.492	3.810E-04	3.580E-04	5.363E-06	3.751E-04	3.644E-04
14.700	3.633E-04	251.817	3.710E-04	3.530E-04	5.430E-06	3.687E-04	3.579E-04
14.800	3.628E-04	252.187	3.820E-04	3.460E-04	8.473E-06	3.713E-04	3.543E-04
14.900	3.641E-04	252.889	3.880E-04	3.480E-04	8.576E-06	3.727E-04	3.556E-04
15.000	3.746E-04	255.233	3.890E-04	3.580E-04	7.794E-06	3.824E-04	3.668E-04
15.100	3.596E-04	253.053	3.750E-04	3.370E-04	8.005E-06	3.676E-04	3.516E-04
15.300	3.159E-04	245.676	3.490E-04	2.840E-04	1.782E-05	3.338E-04	2.981E-04
15.500	2.300E-04	227.770	3.900E-04	7.300E-05	6.165E-05	2.917E-04	1.683E-04

λ = Wavelength (μm)

$\overline{L}$ = Average radiance (W/cm^2 . str . μm)

$\overline{T}_{eff}$ = Effective radiometric temperature (Kelvins)

L_{max} = Maximum observed radiance (W/cm^2 . str . μm)

L_{min} = Minimum observed radiance (W/cm^2 . str. μm)

σ_L = Standard deviation of radiance (W/cm^2 . str . μm)

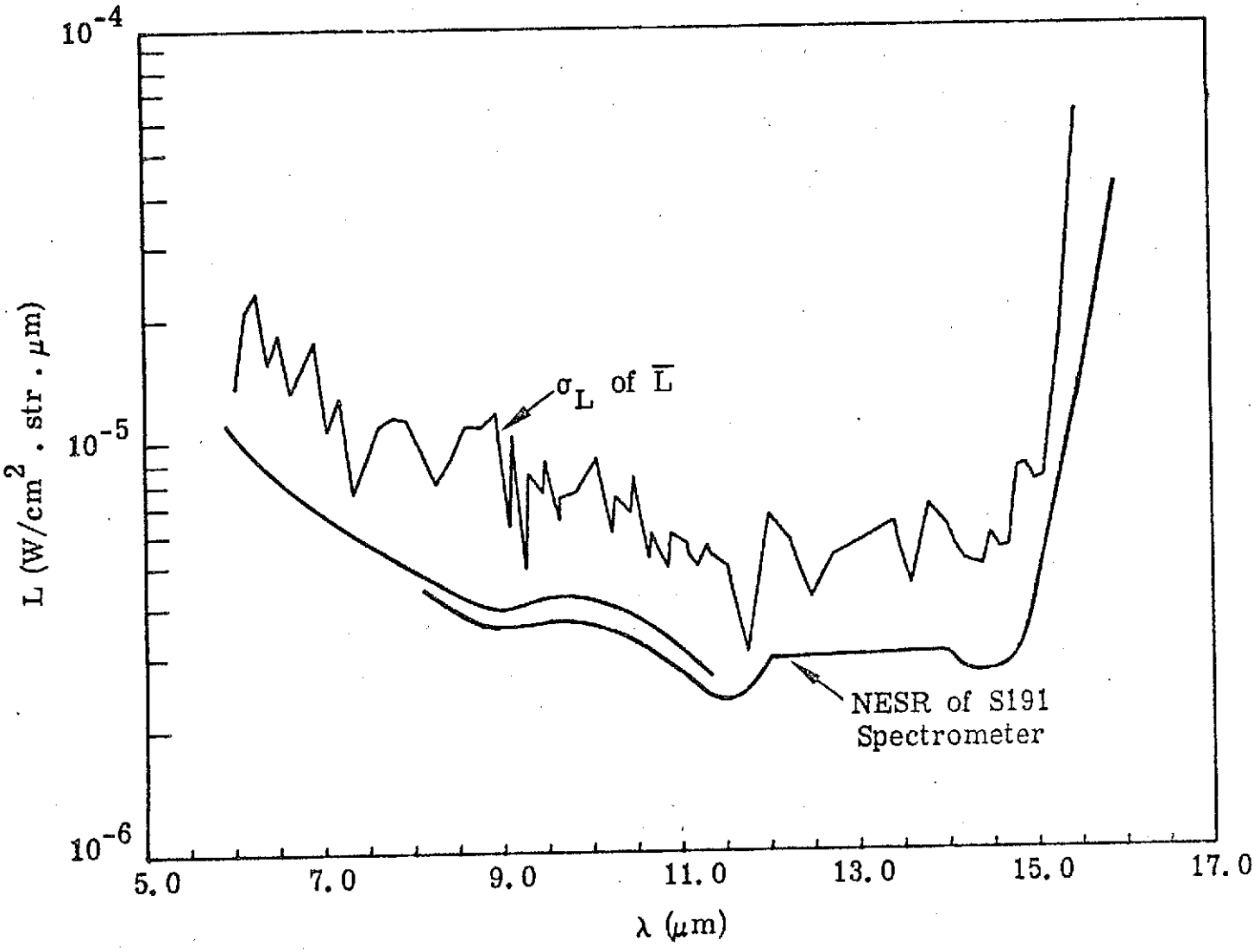

Figure 1. Standard Deviation of Average Radiance Compared to NESR of S191 Spectrometer for SL-2 Pass No. 5.

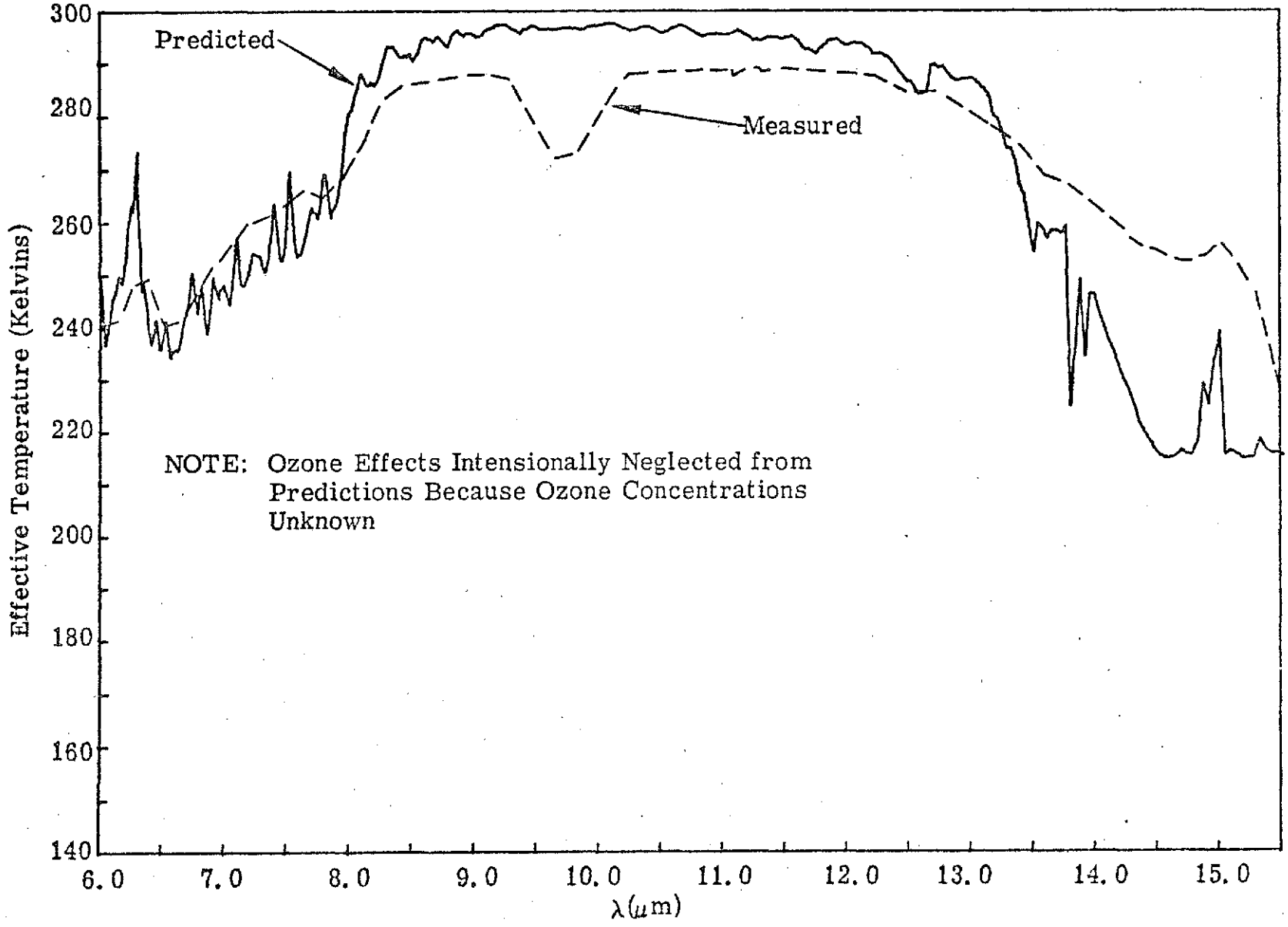

Figure 2. Measured and Predicted Effective Temperature for SL-2 Pass No. 5.

results are shown in figures 3 and 4. These data comprise the model atmosphere that was used as input to the radiative transfer model.

Returning to figure 2, it is observed that the effective radiometric temperatures between 6.0 and 8.0 μm are comparable but are different by approximately 10 Kelvins between 8.0 and 12.0 μm. This discrepancy is too large to be explained by an atmospheric effect or possible errors in the radiative transfer model. A plausible explanation is that the field of view was contaminated by low cumulus clouds causing the observed cooler effective temperatures. A further discrepancy between the observed and predicted values is the unusually high effective temperatures near 15 μm for the S191 data. In a previous statistical study [2] of infrared radiometric data from Nimbus for these latitudes the mean effective temperature in this spectral region was $\sim$224 Kelvins with a plus 2σ temperature of $\sim$229 Kelvins. The observed effective temperature of $\sim$255 Kelvins therefore appears unrealistic and probably is a result of a calibration error.

Additional support data acquired by NOAA satellites is being obtained from E. Paul McClain at the National Environmental Satellite Service (NESS) which will provide further information about possible cloud contamination of the field of view and the temperature of the ocean surface. A judgement concerning the useability of the June 5th S191 data for the planned analysis will be delayed until the NOAA data are received and examined.

SL-2, EREP Pass No. 8

Day of Year: 162, June 11, 1973
Location (approximate): 25N; 87W
GMT Start: 15:21:44
GMT End: 15:23:03
Sun Angle (approximate): 56^{o}

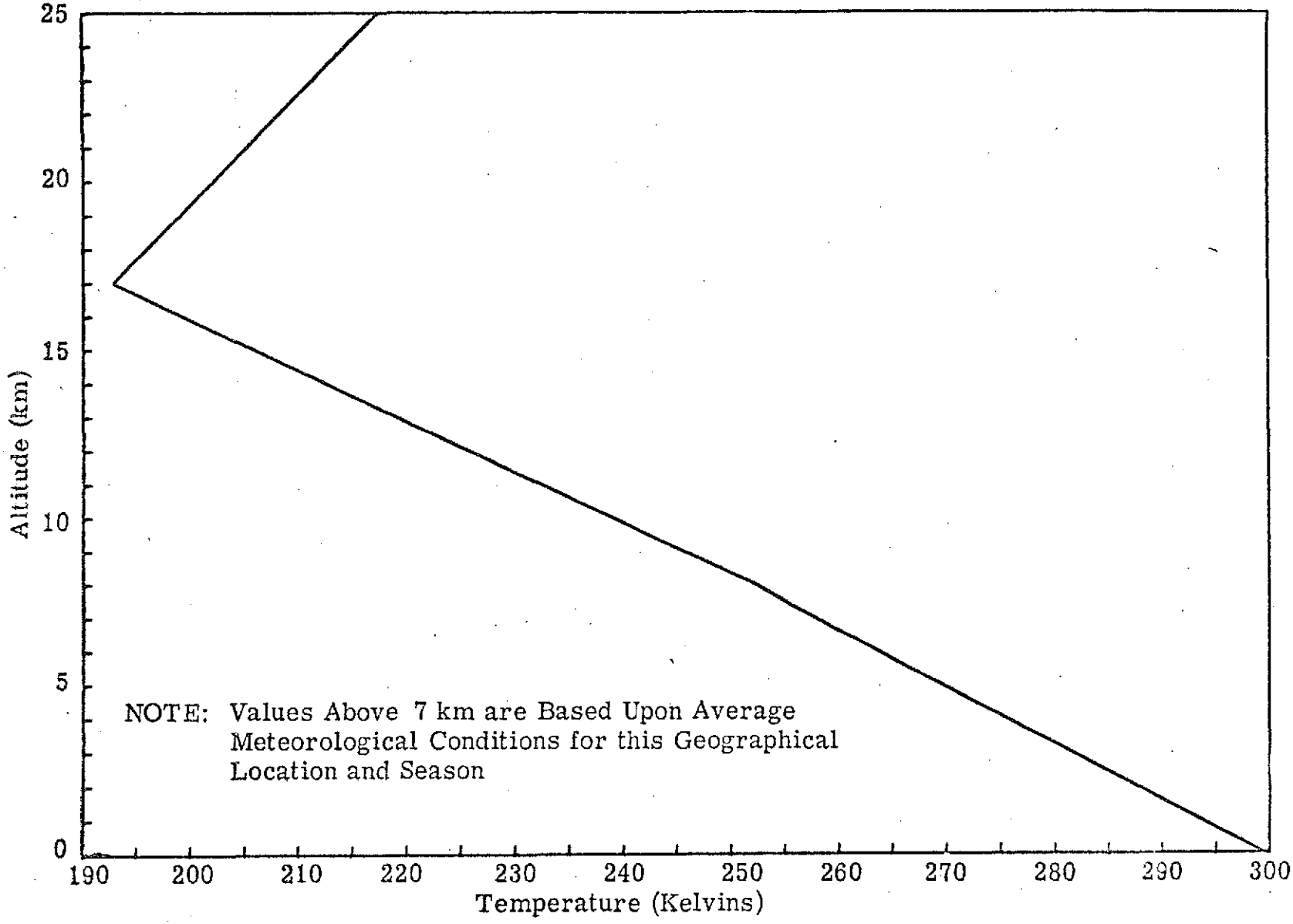

Figure 3. Temperature Distribution along Suborbital Track Measured by NOAA Aircraft During SL-2 Pass No. 5.

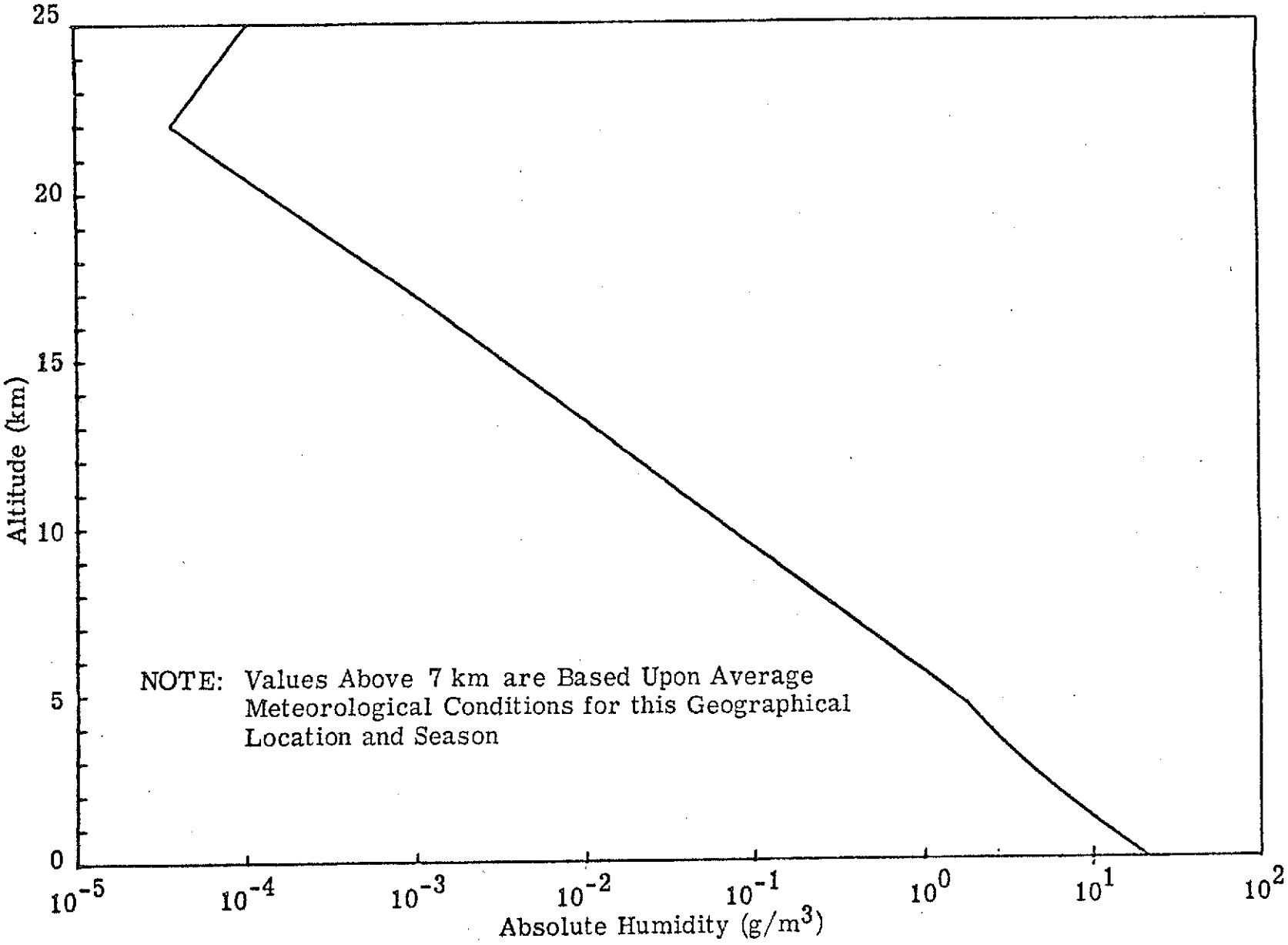

Figure 4. Mean Humidity Distribution along Suborbital Track Measured by NOAA Aircraft during SL-2 Pass No. 5.

Skylab was also in a descending mode on pass 8. V/TS photography indicated that southern Texas and the northern Gulf of Mexico was blanketed by clouds. Cloud conditions reduced to scattered cumulus at 21:42 GMT, the beginning of data acquisition, at approximately 26.472°N latitude and 89.241°W longitude. During the data acquisition period it appeared from the photography that clouds intermittently entered the field of view of the S191, although this was not in evidence in the radiance data (i. e., clouds usually cause observable decreases in radiance which were not noted). Support data is also being obtained from NESS for this region which will hopefully define the cloud conditions of the field of view during the data acquisition period.

In total, approximately 93 spectra were acquired for "apparent" clear conditions and after eliminating those which contained spurious signals 85 remained. These data were statistically processed exactly as those for pass 5 and the results are given in table III. In figure 5 the standard deviation is compared to the NESR For most of the spectral region the variance is slightly larger than that for pass 5 but does not indicate any unusual or identifiable features.* An examination of the effective temperature of the average spectrum does, however, suggest a possible calibration problem. In figure 6 calculations are compared with the measurement data. The calculated values were obtained in an analogous manner to those for pass 5 using air and sea surface temperature data supplied by Duncan Ross. The prevailing atmospheric conditions were almost identical to those of June 5 and the sea surface temperature, again remaining uniform throughout the data acquisition period, was approximately 29.3 ± 0.2°C. The comparison indicates that the effective temperatures are low from 6.0 to approximately 10.0 μm, and are unrealistically low from 6.0 to 8.0 μm since the lowest atmospheric temperatures are approximately 180 Kelvins, some 30 Kelvins warmer than those measured. Assuming the reason for the discrepancy between measured and predicted values is a correctable calibration problem the data should be usable for the planned analysis.

* The low values near 6.3μm result from very low values of absolute radiance.

Table III.

Statistics for SL-2 EREP Pass No. 8, 11 June 1973

λ	$\bar{L}$	$\bar{T}_{eff.}$	$L_{max.}$	$L_{min.}$	σ_L	$\bar{L}+\sigma_L$	$\bar{L}-\sigma_L$
6.020	1.304E-07	146.970	9.000E-06	0.0	1.076E-06	1.206E-06	-9.452E-07
6.140	9.565E-07	165.362	3.300E-05	0.0	4.385E-06	5.342E-06	-3.429E-06
6.260	2.085E-05	209.096	5.000E-05	0.0	1.227E-05	3.312E-05	8.587E-06
6.390	2.155E-05	207.400	5.600E-05	0.0	1.265E-05	3.420E-05	8.902E-06
6.510	1.594E-07	141.042	7.000E-06	0.0	9.109E-07	1.070E-06	-7.514E-07
6.640	3.855E-06	174.950	2.900E-05	0.0	6.309E-06	1.016E-05	-2.454E-06
6.780	3.093E-05	208.070	5.600E-05	0.0	1.050E-05	4.143E-05	2.043E-05
6.910	6.883E-05	223.791	1.000E-04	3.800E-05	1.253E-05	8.135E-05	5.630E-05
7.050	1.212E-04	236.270	1.480E-04	9.400E-05	1.297E-05	1.342E-04	1.083E-04
7.190	1.668E-04	243.427	2.020E-04	1.350E-04	1.467E-05	1.815E-04	1.521E-04
7.340	2.146E-04	249.215	2.490E-04	1.700E-04	1.676E-05	2.313E-04	1.978E-04
7.480	2.613E-04	253.957	2.960E-04	2.180E-04	1.825E-05	2.795E-04	2.431E-04
7.630	3.188E-04	259.160	3.450E-04	2.770E-04	1.796E-05	3.368E-04	3.008E-04
7.790	3.305E-04	258.810	3.580E-04	2.810E-04	1.451E-05	3.450E-04	3.160E-04
7.940	4.019E-04	264.696	4.270E-04	3.510E-04	1.434E-05	4.162E-04	3.875E-04
8.100	5.368E-04	275.091	5.920E-04	4.590E-04	2.533E-05	5.622E-04	5.115E-04
8.260	6.976E-04	285.646	7.280E-04	6.410E-04	1.646E-05	7.141E-04	6.811E-04
8.430	7.719E-04	289.501	7.930E-04	7.260E-04	1.471E-05	7.866E-04	7.572E-04
8.600	7.974E-04	290.279	8.220E-04	7.570E-04	1.430E-05	8.117E-04	7.831E-04
8.770	8.315E-04	291.700	8.570E-04	7.930E-04	1.308E-05	8.446E-04	8.184E-04
8.940	8.540E-04	292.508	8.780E-04	8.080E-04	1.268E-05	8.667E-04	8.413E-04
9.090	8.679E-04	292.947	8.850E-04	8.240E-04	1.202E-05	8.799E-04	8.558E-04
9.120	8.684E-04	292.903	8.890E-04	8.320E-04	1.247E-05	8.808E-04	8.559E-04
9.270	8.671E-04	292.492	8.840E-04	8.270E-04	1.133E-05	8.784E-04	8.558E-04
9.300	8.643E-04	292.256	8.830E-04	8.260E-04	1.120E-05	8.755E-04	8.531E-04
9.460	7.377E-04	283.421	7.720E-04	7.070E-04	1.563E-05	7.533E-04	7.221E-04
9.490	7.054E-04	281.013	7.370E-04	6.760E-04	1.369E-05	7.190E-04	6.917E-04
9.650	6.062E-04	272.930	6.210E-04	5.800E-04	7.959E-06	6.141E-04	5.982E-04
9.650	5.985E-04	272.296	6.130E-04	5.810E-04	8.161E-06	6.066E-04	5.903E-04
9.840	6.256E-04	274.104	6.440E-04	5.940E-04	1.029E-05	6.359E-04	6.153E-04
10.040	7.791E-04	285.692	8.080E-04	7.320E-04	1.351E-05	7.926E-04	7.656E-04
10.070	8.033E-04	287.431	8.270E-04	7.660E-04	1.263E-05	8.160E-04	7.907E-04
10.240	8.954E-04	293.938	9.150E-04	8.490E-04	1.306E-05	9.085E-04	8.824E-04
10.270	8.990E-04	294.218	9.180E-04	8.570E-04	1.239E-05	9.119E-04	8.861E-04
10.440	9.077E-04	295.056	9.260E-04	8.600E-04	1.342E-05	9.211E-04	8.943E-04
10.480	9.084E-04	295.178	9.350E-04	8.630E-04	1.283E-05	9.213E-04	8.956E-04
10.650	9.012E-04	295.019	9.200E-04	8.400E-04	1.452E-05	9.158E-04	8.867E-04
10.680	9.034E-04	295.241	9.220E-04	8.540E-04	1.302E-05	9.164E-04	8.904E-04
10.870	8.928E-04	294.964	9.110E-04	8.320E-04	1.459E-05	9.074E-04	8.782E-04
10.900	8.934E-04	295.090	9.130E-04	8.410E-04	1.342E-05	9.068E-04	8.800E-04
11.080	8.808E-04	294.702	9.030E-04	8.180E-04	1.516E-05	8.959E-04	8.656E-04
11.100	8.813E-04	294.804	9.030E-04	8.410E-04	1.289E-05	8.942E-04	8.684E-04
11.200	8.740E-04	294.594	8.940E-04	8.400E-04	1.185E-05	8.859E-04	8.622E-04
11.310	8.696E-04	294.650	8.880E-04	8.160E-04	1.512E-05	8.847E-04	8.545E-04
11.350	8.481E-04	293.114	8.660E-04	8.070E-04	1.184E-05	8.599E-04	8.362E-04
11.530	8.558E-04	294.429	8.720E-04	8.020E-04	1.309E-05	8.709E-04	8.407E-04
11.760	8.321E-04	293.492	8.520E-04	7.850E-04	1.435E-05	8.465E-04	8.178E-04

Table III. (Continued)

λ	$\overline{L}$	$\overline{T}_{eff.}$	$L_{max.}$	$L_{min.}$	σ_L	$\overline{L}+\sigma_L$	$\overline{L}-\sigma_L$
12.000	8.224E-04	293.813	8.410E-04	7.690E-04	1.463E-05	8.370E-04	8.078E-04
12.240	7.966E-04	292.781	8.140E-04	7.490E-04	1.452E-05	8.111E-04	7.820E-04
12.480	7.429E-04	289.087	7.710E-04	7.010E-04	1.391E-05	7.568E-04	7.290E-04
12.730	7.290E-04	289.118	7.500E-04	6.890E-04	1.254E-05	7.416E-04	7.165E-04
13.400	5.548E-04	273.521	5.760E-04	5.200E-04	1.097E-05	5.658E-04	5.438E-04
13.600	4.766E-04	264.359	4.870E-04	4.590E-04	6.926E-06	4.836E-04	4.697E-04
13.800	4.458E-04	260.922	4.590E-04	4.320E-04	5.998E-06	4.518E-04	4.398E-04
14.000	3.855E-04	252.640	3.980E-04	3.750E-04	5.132E-06	3.907E-04	3.804E-04
14.100	3.591E-04	248.713	3.740E-04	3.500E-04	5.031E-06	3.641E-04	3.540E-04
14.200	3.239E-04	243.017	3.380E-04	3.150E-04	5.395E-06	3.293E-04	3.185E-04
14.300	2.829E-04	235.720	2.940E-04	2.710E-04	4.470E-06	2.873E-04	2.784E-04
14.400	2.494E-04	229.260	2.570E-04	2.420E-04	3.376E-06	2.528E-04	2.460E-04
14.500	2.259E-04	224.404	2.330E-04	2.200E-04	2.777E-06	2.287E-04	2.231E-04
14.600	2.124E-04	221.516	2.200E-04	2.070E-04	2.910E-06	2.153E-04	2.095E-04
14.700	2.037E-04	219.628	2.100E-04	1.960E-04	3.133E-06	2.068E-04	2.005E-04
14.800	1.942E-04	217.480	2.040E-04	1.860E-04	3.552E-06	1.977E-04	1.906E-04
14.900	1.973E-04	218.426	2.130E-04	1.840E-04	5.466E-06	2.028E-04	1.919E-04
15.000	2.036E-04	220.154	2.160E-04	1.950E-04	4.767E-06	2.084E-04	1.989E-04
15.100	2.020E-04	219.949	2.130E-04	1.940E-04	3.351E-06	2.053E-04	1.986E-04
15.300	1.621E-04	209.702	1.750E-04	1.450E-04	6.546E-06	1.686E-04	1.556E-04
15.500	9.694E-05	188.306	1.230E-04	7.500E-05	1.130E-05	1.082E-04	8.564E-05

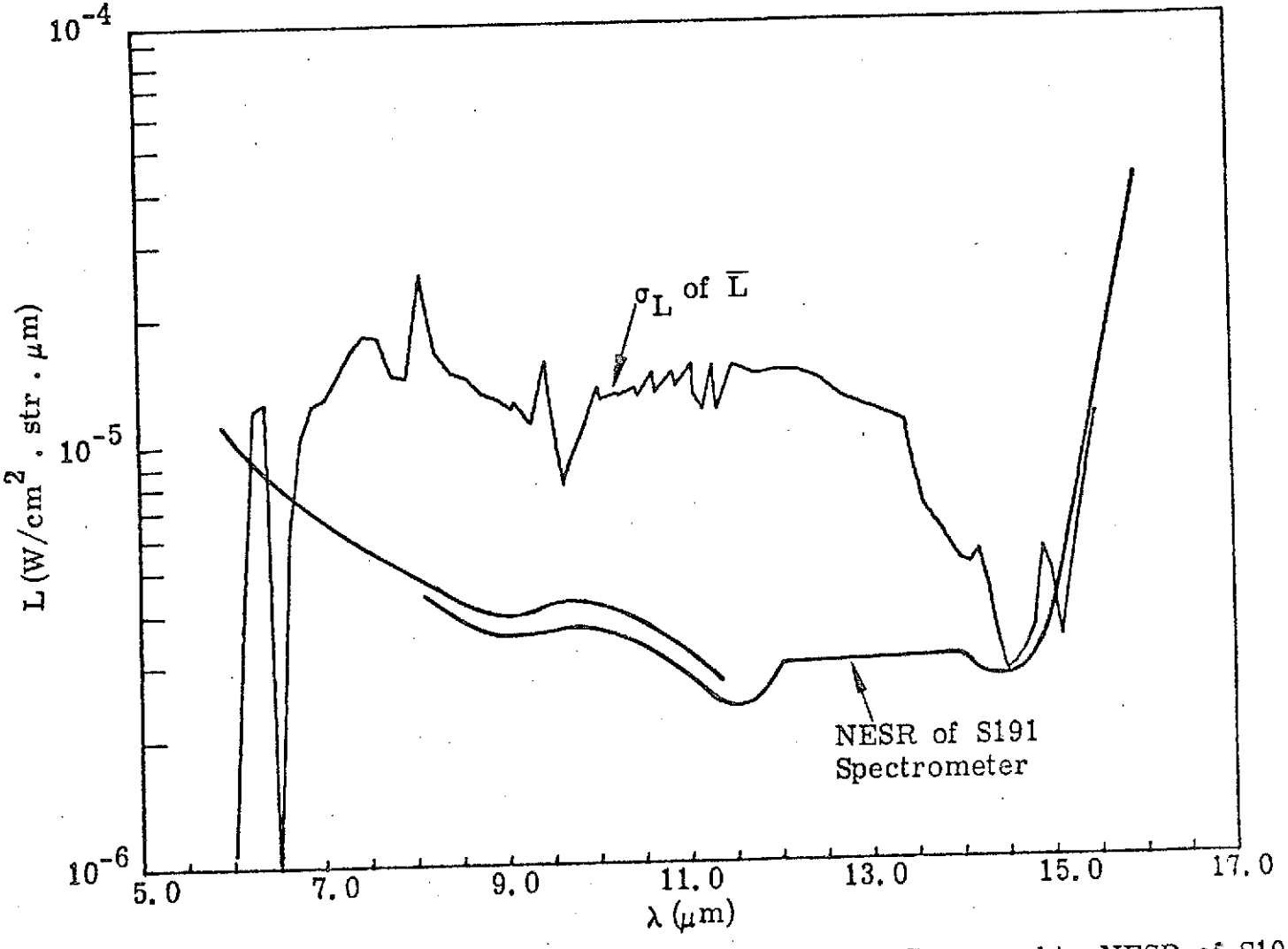

Figure 5. Standard Deviation of Average Radiance Compared to NESR of S191 Spectrometer for SL-2 Pass No. 8.

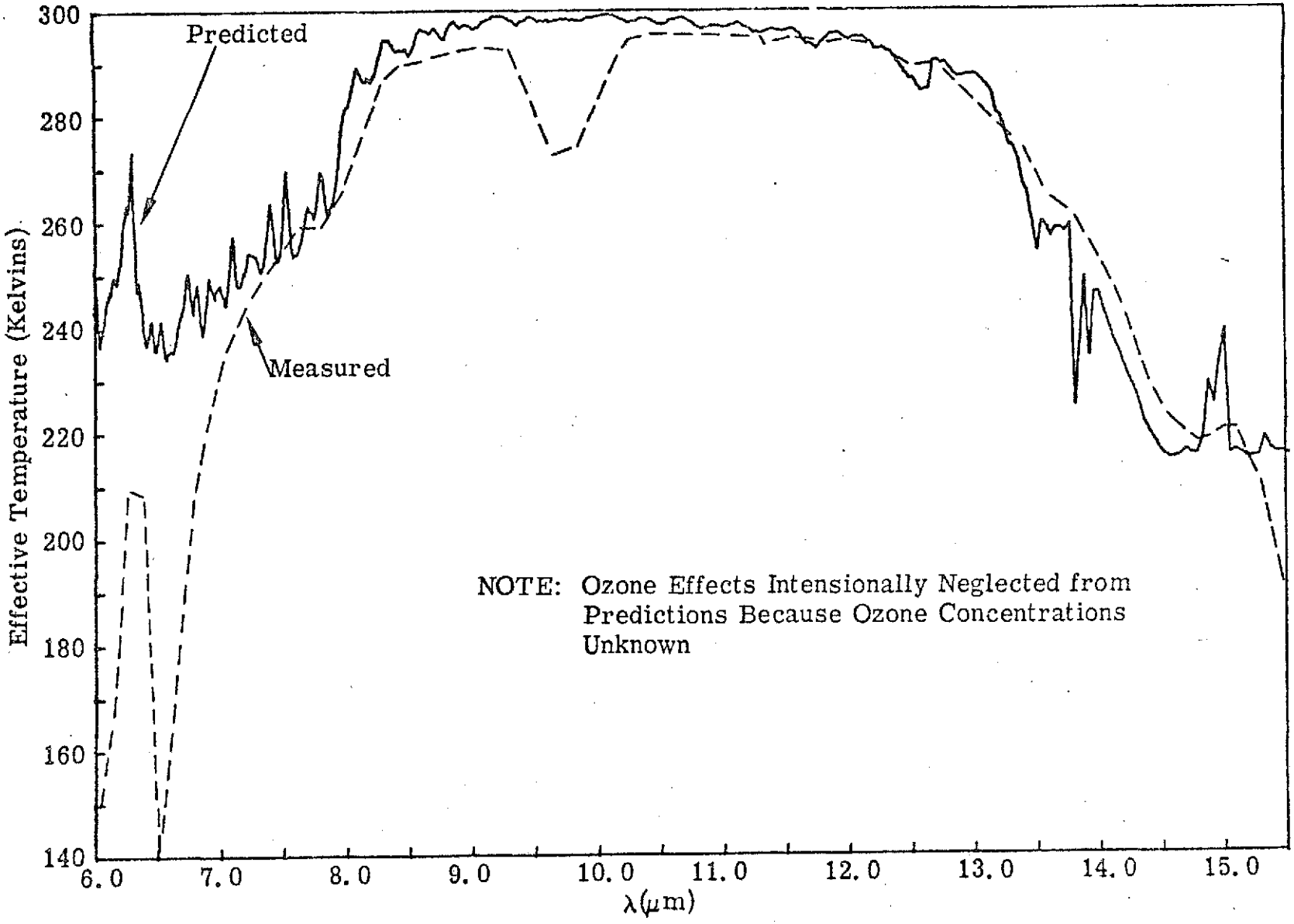

Figure 6. Measured and Predicted Effective Temperature for SL-2 Pass No. 8.

SL-3, EREP Pass No. 16

Day of Year: 220, August 8, 1973
Location (approximate): 45.27N; 125.28W
GMT Start: 15:57:19
GMT End: 15:58:49
Sun Angle (approximate): 23^{o}

The relevant test site for this orbital pass was a low-altitude coastal-stratus cloud deck off the coast of Oregon. The cloud deck was encountered at approximately 15:57:19 GMT, 45 degrees forward of the spacecraft, and tracked to 11^{o} aft. During this time spectra were acquired. Examination of the V/TS photography revealed that the visual brightness of the cloud deck remained very uniform throughout the tracking period and that it was a particularly good acquisition and track. This fact is substantiated by a consistent and predictable set of spectral data. As for the previous data sets the mean and variance of the data were calculated. The results are given in table IV. The standard deviation is shown in figure 7 and displays a noteworthy phenomena. Near each of the absorption bands (i. e., 6.3 μm H_2O, 9.6 μm O_3, and 15 μm CO_2) the variance increases significantly from the values for the window region. This occurs because the spectra were acquired at different viewing angles ranging from 45^{o} forward to 11^{o} aft, and because the effect of the atmosphere on the observed radiance is different for each viewing angle, being greater in the absorption bands than in the window regions.

Although the data appear to be of high quality an examination of the effective temperature of the average spectrum, shown in figure 8, reveals unrealistically low values of radiance from 6.0 to approximately 8.0 μm and slightly low values between 8.0 and 11.0 μm. Since there was no air truth available for these data the calculated values were based upon mean atmospheric conditions for the latitude and season represented and a cloud top altitude which yielded comparable radiance at 11.0 μm. Since clouds are approximately blackbody radiators in the window regions the effective

Table IV.

Statistics for SL-3 EREP Pass No. 16, 8 August 1973

λ	$\overline{L}$	$\overline{T}_{eff.}$	$L_{max.}$	$L_{min.}$	σ_L	$\overline{L}+\sigma_L$	$\overline{L}-\sigma_L$
6.020	7.968E-06	196.715	3.700E-05	0.0	9.208E-06	1.718E-05	-1.240E-06
6.140	1.008E-05	198.321	3.700E-05	0.0	9.794E-06	1.987E-05	2.863E-07
6.260	3.642E-05	220.263	7.100E-05	0.0	1.338E-05	4.980E-05	2.304E-05
6.390	3.291E-05	215.817	7.100E-05	0.0	1.317E-05	4.608E-05	1.974E-05
6.510	8.573E-06	189.138	3.800E-05	0.0	9.408E-06	1.798E-05	-8.359E-07
6.640	2.904E-05	209.029	5.300E-05	4.000E-06	9.921E-06	3.896E-05	1.912E-05
6.780	6.346E-05	223.844	9.600E-05	3.700E-05	1.097E-05	7.443E-05	5.249E-05
6.910	1.023E-04	233.758	1.250E-04	7.100E-05	1.115E-05	1.135E-04	9.120E-05
7.050	1.512E-04	242.470	1.840E-04	1.200E-04	1.316E-05	1.644E-04	1.381E-04
7.190	1.940E-04	247.981	2.300E-04	1.520E-04	1.443E-05	2.084E-04	1.796E-04
7.340	2.339E-04	251.970	2.740E-04	1.910E-04	1.479E-05	2.487E-04	2.191E-04
7.480	2.679E-04	254.801	3.040E-04	2.260E-04	1.695E-05	2.849E-04	2.510E-04
7.630	3.128E-04	258.482	3.430E-04	2.690E-04	1.638E-05	3.291E-04	2.964E-04
7.790	3.093E-04	256.423	3.390E-04	2.710E-04	1.700E-05	3.263E-04	2.923E-04
7.940	3.623E-04	260.751	3.980E-04	3.120E-04	1.795E-05	3.802E-04	3.443E-04
8.100	4.648E-04	269.093	5.020E-04	4.290E-04	1.391E-05	4.787E-04	4.509E-04
8.260	5.715E-04	276.623	5.900E-04	5.450E-04	7.324E-06	5.789E-04	5.642E-04
8.430	6.042E-04	277.979	6.230E-04	5.870E-04	7.700E-06	6.119E-04	5.965E-04
8.600	6.146E-04	277.760	6.310E-04	5.950E-04	7.381E-06	6.219E-04	6.072E-04
8.770	6.245E-04	277.610	6.410E-04	5.970E-04	7.751E-06	6.322E-04	6.167E-04
8.940	6.328E-04	277.443	6.500E-04	6.150E-04	7.339E-06	6.401E-04	6.254E-04
9.090	6.535E-04	278.385	6.750E-04	6.360E-04	6.912E-06	6.604E-04	6.466E-04
9.120	6.484E-04	277.894	6.690E-04	6.280E-04	7.604E-06	6.560E-04	6.408E-04
9.270	6.609E-04	278.315	6.820E-04	6.460E-04	6.743E-06	6.677E-04	6.542E-04
9.300	6.554E-04	277.805	6.770E-04	6.380E-04	7.562E-06	6.630E-04	6.479E-04
9.460	5.940E-04	272.465	6.210E-04	5.630E-04	1.139E-05	6.054E-04	5.826E-04
9.490	5.511E-04	268.772	5.840E-04	5.230E-04	1.501E-05	5.662E-04	5.361E-04
9.650	4.807E-04	261.861	5.030E-04	4.530E-04	1.427E-05	4.950E-04	4.665E-04
9.650	4.692E-04	260.750	4.970E-04	4.410E-04	1.546E-05	4.846E-04	4.537E-04
9.840	4.840E-04	261.574	5.120E-04	4.500E-04	1.586E-05	4.998E-04	4.681E-04
10.040	5.831E-04	270.172	6.100E-04	5.460E-04	1.104E-05	5.942E-04	5.721E-04
10.070	6.012E-04	271.683	6.220E-04	5.780E-04	1.049E-05	6.117E-04	5.907E-04
10.240	6.930E-04	279.087	7.080E-04	6.780E-04	6.528E-06	6.995E-04	6.865E-04
10.270	6.951E-04	279.243	7.210E-04	6.780E-04	7.677E-06	7.028E-04	6.874E-04
10.440	7.130E-04	281.063	7.390E-04	7.070E-04	6.023E-06	7.240E-04	7.119E-04
10.480	7.150E-04	280.845	7.470E-04	6.980E-04	7.632E-06	7.227E-04	7.074E-04
10.650	7.235E-04	281.632	7.400E-04	7.130E-04	5.482E-06	7.289E-04	7.180E-04
10.680	7.200E-04	281.382	7.420E-04	7.080E-04	6.368E-06	7.264E-04	7.137E-04
10.870	7.276E-04	282.225	7.470E-04	7.180E-04	5.845E-06	7.334E-04	7.217E-04
10.900	7.212E-04	281.748	7.450E-04	7.080E-04	5.821E-06	7.271E-04	7.154E-04
11.080	7.295E-04	282.747	7.470E-04	7.180E-04	5.680E-06	7.352E-04	7.238E-04
11.100	7.228E-04	282.221	7.410E-04	7.060E-04	5.838E-06	7.286E-04	7.169E-04
11.200	7.310E-04	283.129	7.490E-04	7.210E-04	4.794E-06	7.358E-04	7.262E-04
11.310	7.297E-04	283.279	7.460E-04	7.210E-04	4.302E-06	7.340E-04	7.254E-04
11.350	7.208E-04	282.616	7.330E-04	7.120E-04	3.923E-06	7.247E-04	7.169E-04
11.530	7.294E-04	283.867	7.410E-04	7.210E-04	3.761E-06	7.332E-04	7.256E-04
11.760	7.207E-04	283.843	7.310E-04	7.110E-04	3.657E-06	7.243E-04	7.170E-04

Table IV. (Continued)

λ	$\bar{L}$	$\bar{T}_{eff.}$	$L_{max.}$	$L_{min.}$	σ_L	$\bar{L}+\sigma_L$	$\bar{L}-\sigma_L$
12.000	7.106E-04	283.807	7.220E-04	7.000E-04	4.262E-06	7.148E-04	7.063E-04
12.240	6.943E-04	283.253	7.050E-04	6.860E-04	3.912E-06	6.982E-04	6.904E-04
12.480	6.697E-04	281.877	6.830E-04	6.590E-04	4.055E-06	6.737E-04	6.656E-04
12.730	6.541E-04	281.461	6.680E-04	6.420E-04	4.233E-06	6.584E-04	6.499E-04
13.400	5.140E-04	268.398	5.350E-04	4.870E-04	1.153E-05	5.255E-04	5.025E-04
13.600	4.521E-04	260.978	4.760E-04	4.240E-04	1.383E-05	4.660E-04	4.383E-04
13.800	4.267E-04	258.146	4.470E-04	4.010E-04	1.330E-05	4.400E-04	4.134E-04
14.000	3.774E-04	251.352	3.990E-04	3.550E-04	1.191E-05	3.885E-04	3.664E-04
14.100	3.569E-04	248.356	3.780E-04	3.370E-04	1.094E-05	3.679E-04	3.460E-04
14.200	3.305E-04	244.168	3.500E-04	3.120E-04	8.953E-06	3.394E-04	3.215E-04
14.300	3.003E-04	239.018	3.140E-04	2.870E-04	5.710E-06	3.060E-04	2.946E-04
14.400	2.804E-04	235.496	2.880E-04	2.720E-04	2.883E-06	2.832E-04	2.775E-04
14.500	2.665E-04	233.010	2.750E-04	2.590E-04	3.502E-06	2.700E-04	2.630E-04
14.600	2.572E-04	231.339	2.680E-04	2.470E-04	4.467E-06	2.617E-04	2.527E-04
14.700	2.485E-04	229.762	2.630E-04	2.370E-04	6.234E-06	2.548E-04	2.423E-04
14.800	2.394E-04	228.011	2.570E-04	2.270E-04	6.217E-06	2.456E-04	2.331E-04
14.900	2.417E-04	228.773	2.580E-04	2.270E-04	6.965E-06	2.486E-04	2.347E-04
15.000	2.447E-04	229.698	2.580E-04	2.290E-04	6.889E-06	2.515E-04	2.378E-04
15.100	2.409E-04	229.130	2.550E-04	2.230E-04	7.003E-06	2.479E-04	2.339E-04
15.300	2.065E-04	221.505	2.280E-04	1.910E-04	8.807E-06	2.153E-04	1.977E-04
15.500	1.550E-04	207.907	1.840E-04	1.170E-04	1.294E-05	1.679E-04	1.420E-04

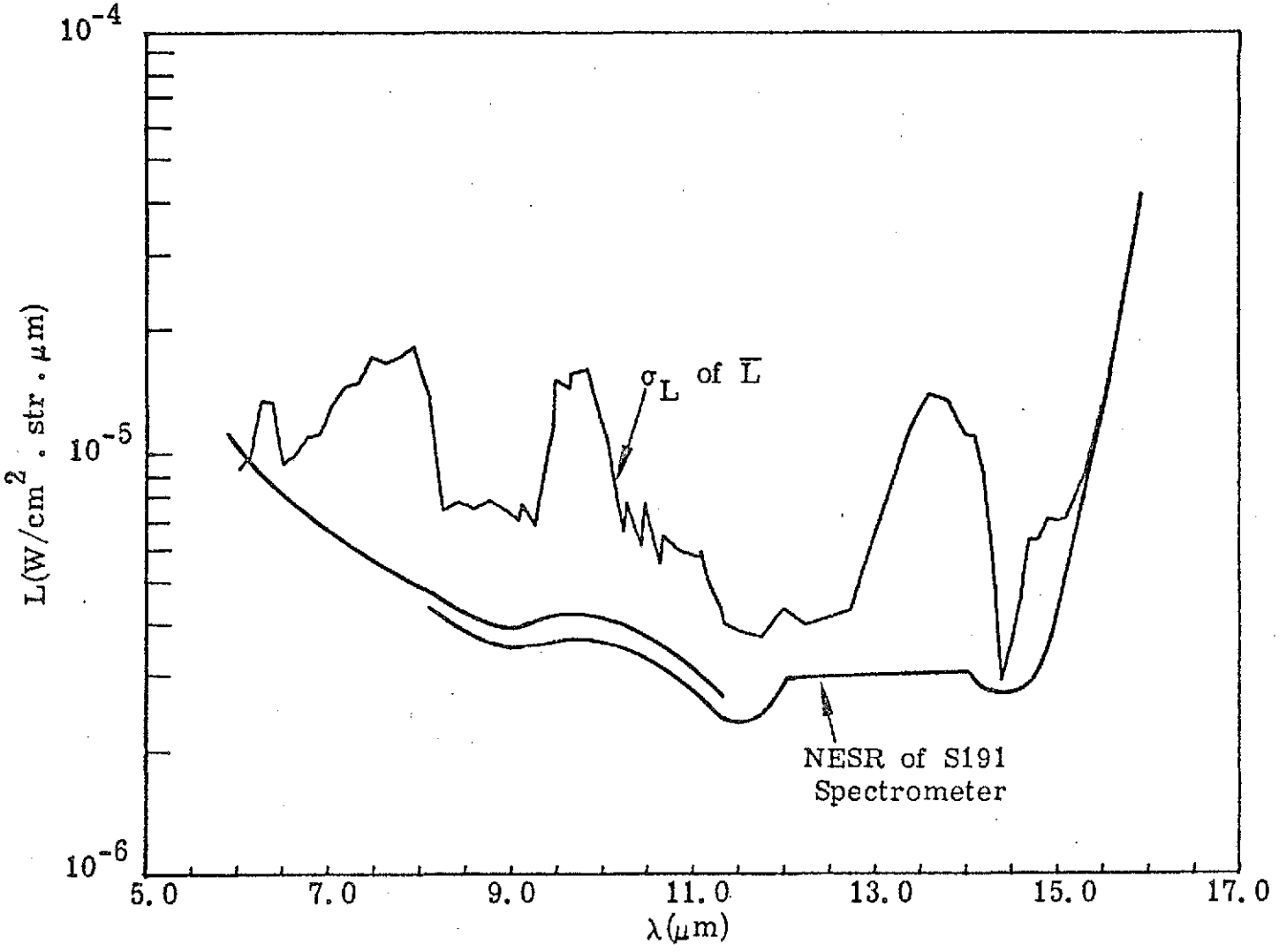

Figure 7. Standard Deviation of Average Radiance Compared to NESR of S191 Spectrometer for SL-3 Pass No. 16.

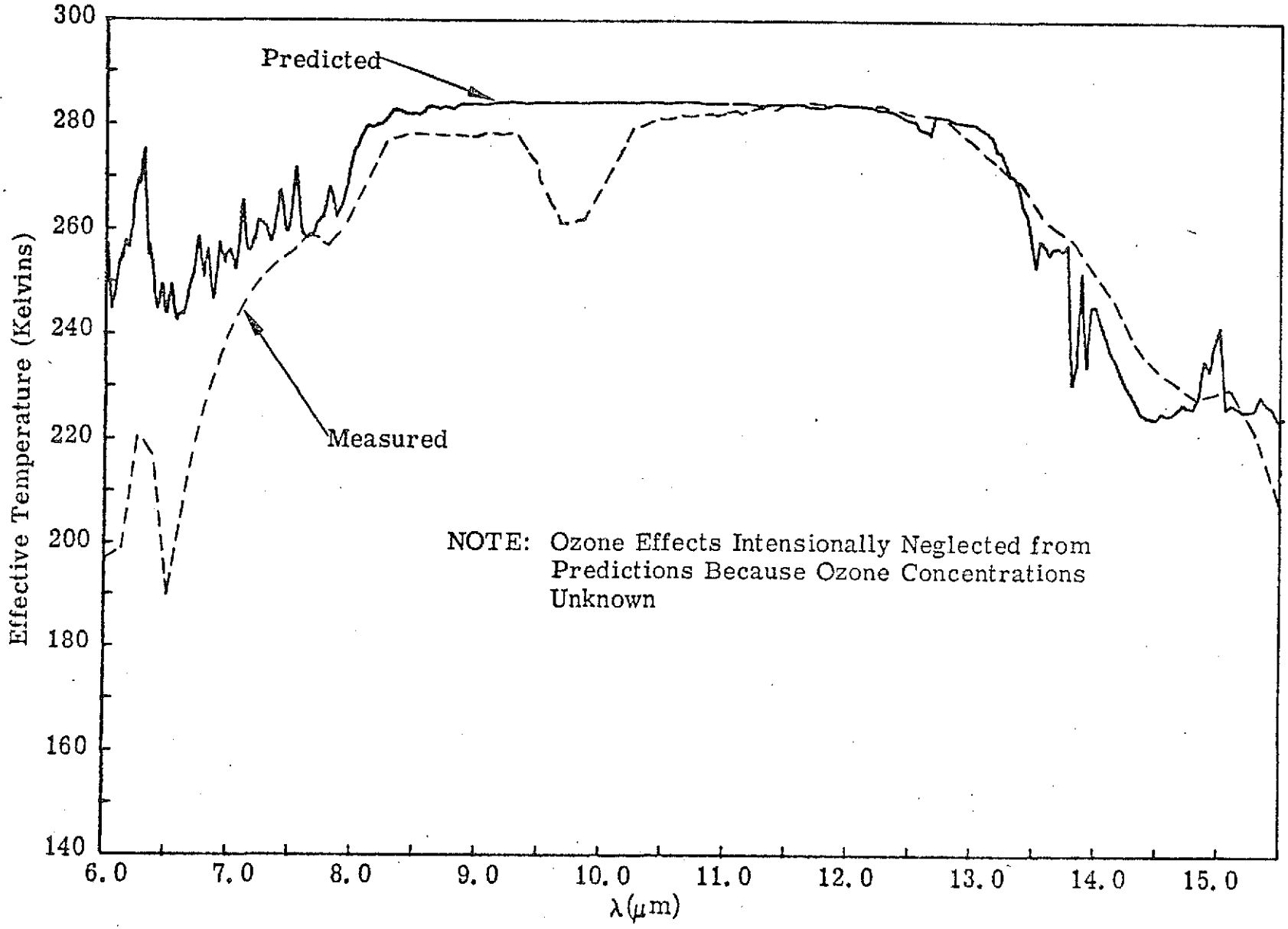

Figure 8. Measured and Predicted Effective Temperature for SL-3 Pass No. 16.

temperatures near 9 and 11 μm should be nearly equal. Differences of 2 Kelvins may be possible because of minor differences in atmospheric effects in the respective regions and minor differences in emissivity, but the nearly 6 Kelvin difference does not appear reasonable. This fact, coupled with the unrealistically low values in the 6.3 μm band, suggest a possible calibration problem. The results in evidence here are almost exactly the same as those indicated by the data from EREP pass No. 8. However, assuming the problem is correctable, the data will be usable for the planned analysis.

SL-3, EREP Pass No. 36

Day of Year: 255, September 12, 1973
Location (approximate): 37.0N; 76.2W
GMT Start: 17:08:20
GMT End: 17:09:33
Sun Angle (approximate): 57^{o}

The target area for this pass was the water surface in Chesapeake Bay. The target was acquired at 45^{o} forward of the spacecraft and tracked to nadir. From the V/TS photography the area appeared cloud free but very hazy. Although the target was tracked for approximately 74 seconds only 11 spectra were obtained. Unfortunately, all spectra contained excessive amounts of spurious signals and are therefore unusable for purposes of the present analysis.

SL-3, EREP Pass No. 43

Day of Year: 258, September 15, 1973
Location (approximate): 27.4N; 123.0W
GMT Start: 18:01:49
GMT End: 18:03:32
Sun Angle (approximate): 51^{o}

The target area for pass 43 was low coastal stratus clouds off the California coast. The target area was acquired at 44^{o} forward of the

spacecraft and tracked to 20^{o} aft during which time 110 spectra were acquired. It appeared to be a good acquisition and track, however, the cloud tops within the field of view did not appear very uniform in brightness or altitude. Although nonuniform, there were no identifiable changes in the appearance of clouds throughout the tracking period.

Unfortunately, the data are not usable in their present form because of apparent calibration problems. This is evidenced in figure 9 where two spectra are displayed, the top one selected from the first part of the data-take period and the bottom one from the latter part. Observe that even initially the values are significantly too low throughout most of the spectral region and there is obviously a loss of calibration near the end of the data-take period. There are a number of indicators that suggest that the data may be usable if the calibration can be corrected; however, this cannot be conclusively determined until the corrected data are received and analyzed.

SL-3, EREP Pass No. 46

Day of Year: 260, September 17, 1973
Location (approximate): 37.6N; 76.6W
GMT Start: 15:06:54
GMT End: 15:07:00
Solar Angle (approximate): 46^{o}

The water surface near the mouth of the Rappahannock River was the relevant target area for pass 46. The area was acquired near 45^{o} forward of the spacecraft and tracked. During the data-take period inspection of the V/TS photography indicated that the field of view appeared contaminated by clouds. This fact is supported by ground observations at the time of data acquisition. Further evidence of cloud contamination is in the data itself. On location water temperature measurements yielded a water temperature ranging from 23 to 25^{o}C. These temperatures, translated into effective temperatures that would be observed by the S191, are approximately 294 Kelvins. Figure 10 shows the average value of the measured radiance

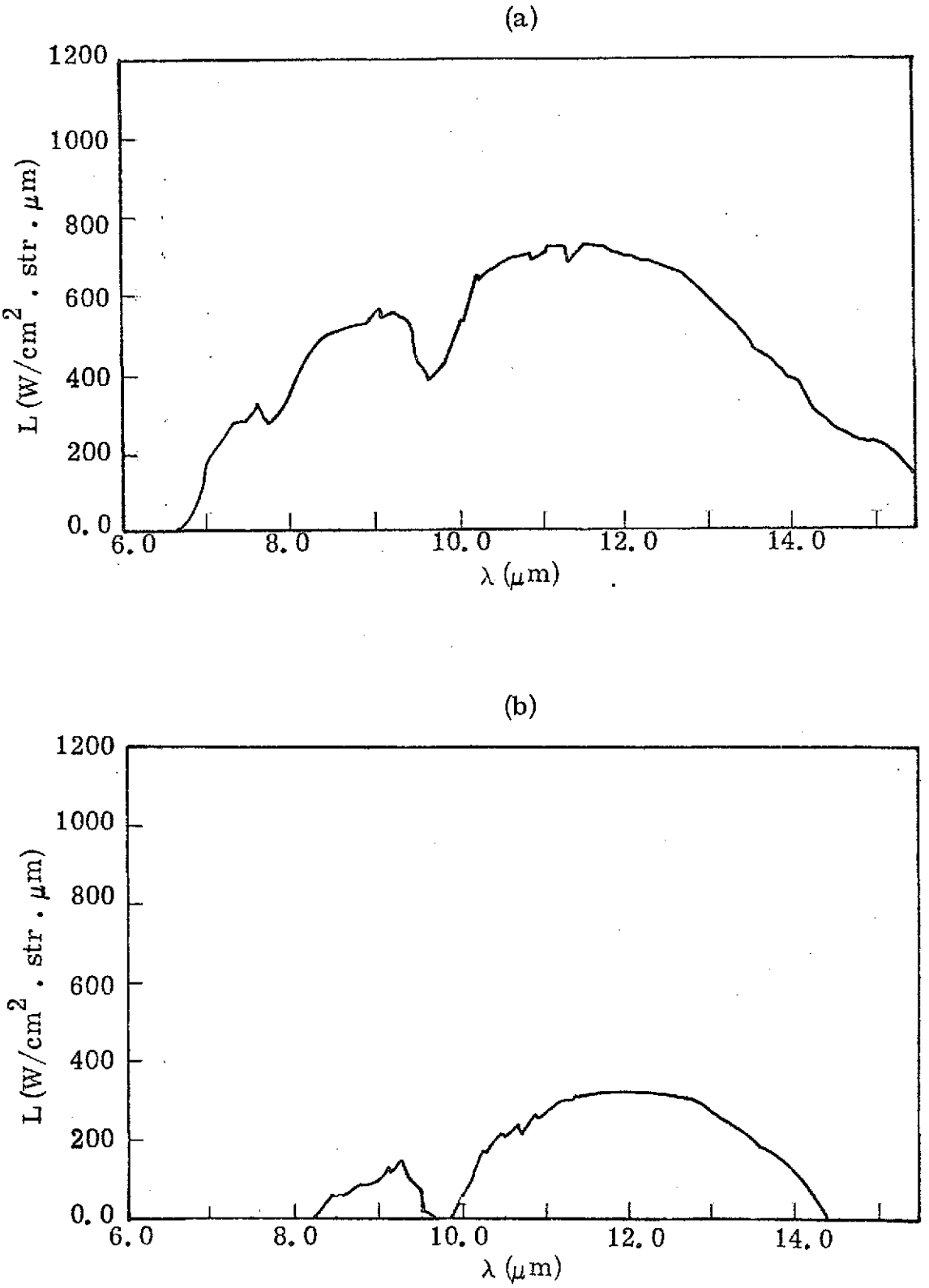

Figure 9. S191 Spectral Radiance at Beginning (a) and End (b) of Cloud Acquisition for SL-3 Pass No. 43.

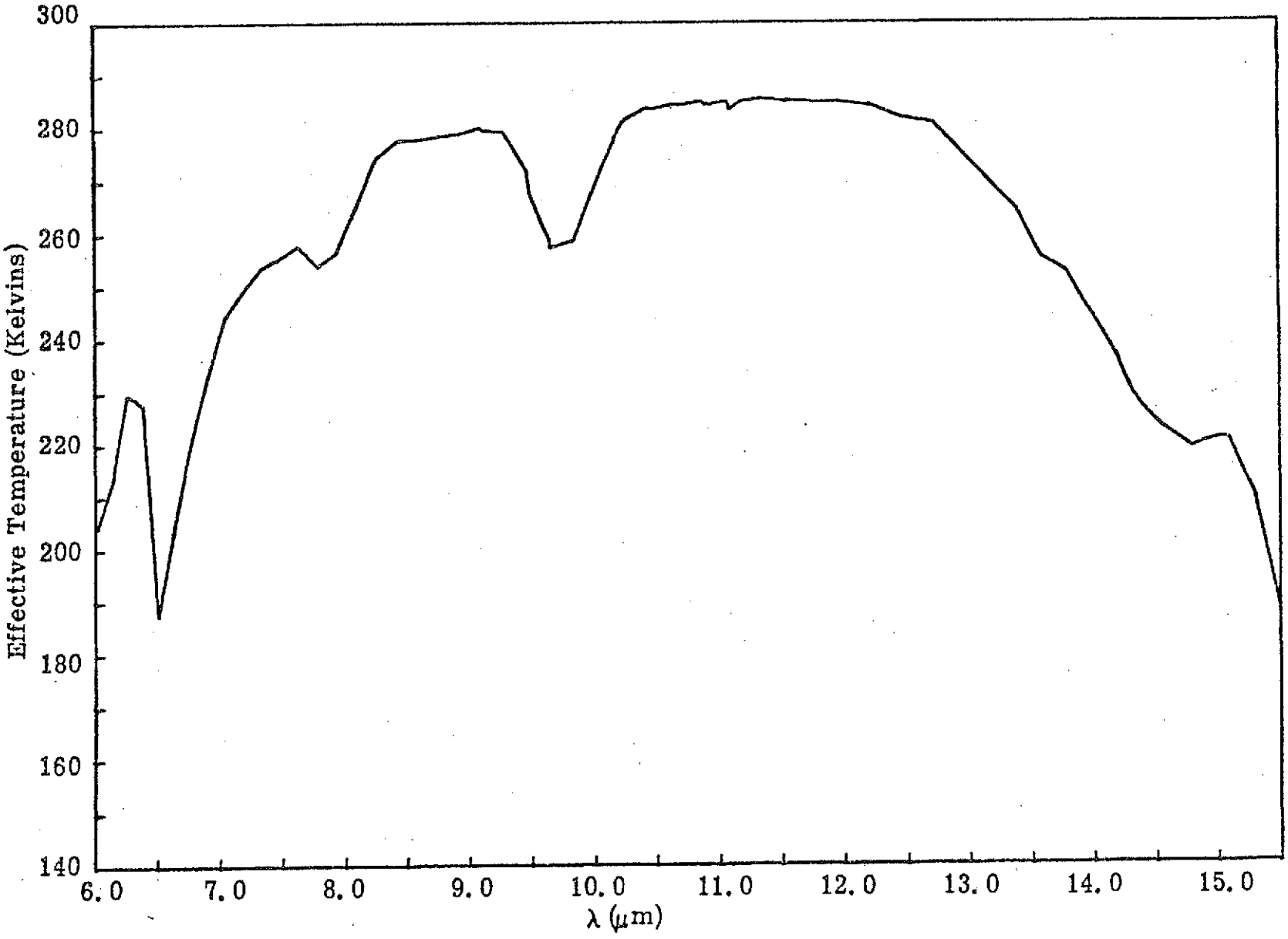

Figure 10. Effective Temperature for SL-3 Pass No. 46.

expressed in terms of effective brightness temperature. Note that the maximum temperature is approximately 284, 10 degrees cooler than that expected. Because of the apparent cloud contamination these data cannot be used for the present analysis.

SUMMARY AND CONCLUSIONS

All of the data received from SL-2 and SL-3 missions were carefully examined and it was found that the data for every test site area contained some irregularities ranging from cloud contamination of the field of view for clear test sites to calibration problems. Of the six sets of data received it appears that the data for passes 5, 36, and 46 cannot be used; because of cloud contamination of the field of view for passes 5 and 46, and because of spurious noise signals for pass 36. The data for the remaining three passes can be used assuming the suspected calibration errors can be corrected.

Future plans include analyzing the corrected data from SL-2 and SL-3 and the data from SL-4 according to the analysis plan discussed in the first quarterly report. The relevant data from SL-4 were acquired on January 8 and January 21 in the vicinity of the Florida Keys. George Maul of NOAA obtained air and surface truth which will provide the environmental data required for the analysis.

REFERENCES

1. D. C. Anding, Use of Skylab Data in a Sea Surface Temperature Experiment, First Quarterly Report, Science Applications, Inc., Ann Arbor, MI, May 1973.

2. H. Rose, D. Anding, J. Walker, R. Kauth, Handbook of Albedo and Thermal Earthshine, Environmental Research Institue of Michigan, Ann Arbor, Michigan, June 1973.